nature structural & molecular biology

SUPPLEMENTARY INFORMATION

https://doi.org/10.1038/s41594-018-0151-4

In the format provided by the authors and unedited.

High-resolution crystal structure of parathyroid hormone 1 receptor in complex with a peptide agonist

Janosch Ehrenmann[1,4], Jendrik Schöppe[1,4], Christoph Klenk[1,4]*, Mathieu Rappas[2], Lutz Kummer[1,3], Andrew S. Doré[2] and Andreas Plückthun[1]*

[1]Department of Biochemistry, University of Zürich, Zurich, Switzerland. [2]Sosei Heptares, Granta Park, Cambridge, UK. [3]Present address: Heptares Therapeutics Zürich AG, Schlieren, Switzerland. [4]These authors contributed equally: Janosch Ehrenmann, Jendrik Schöppe and Christoph Klenk.
*e-mail: c.klenk@bioc.uzh.ch; plueckthun@bioc.uzh.ch

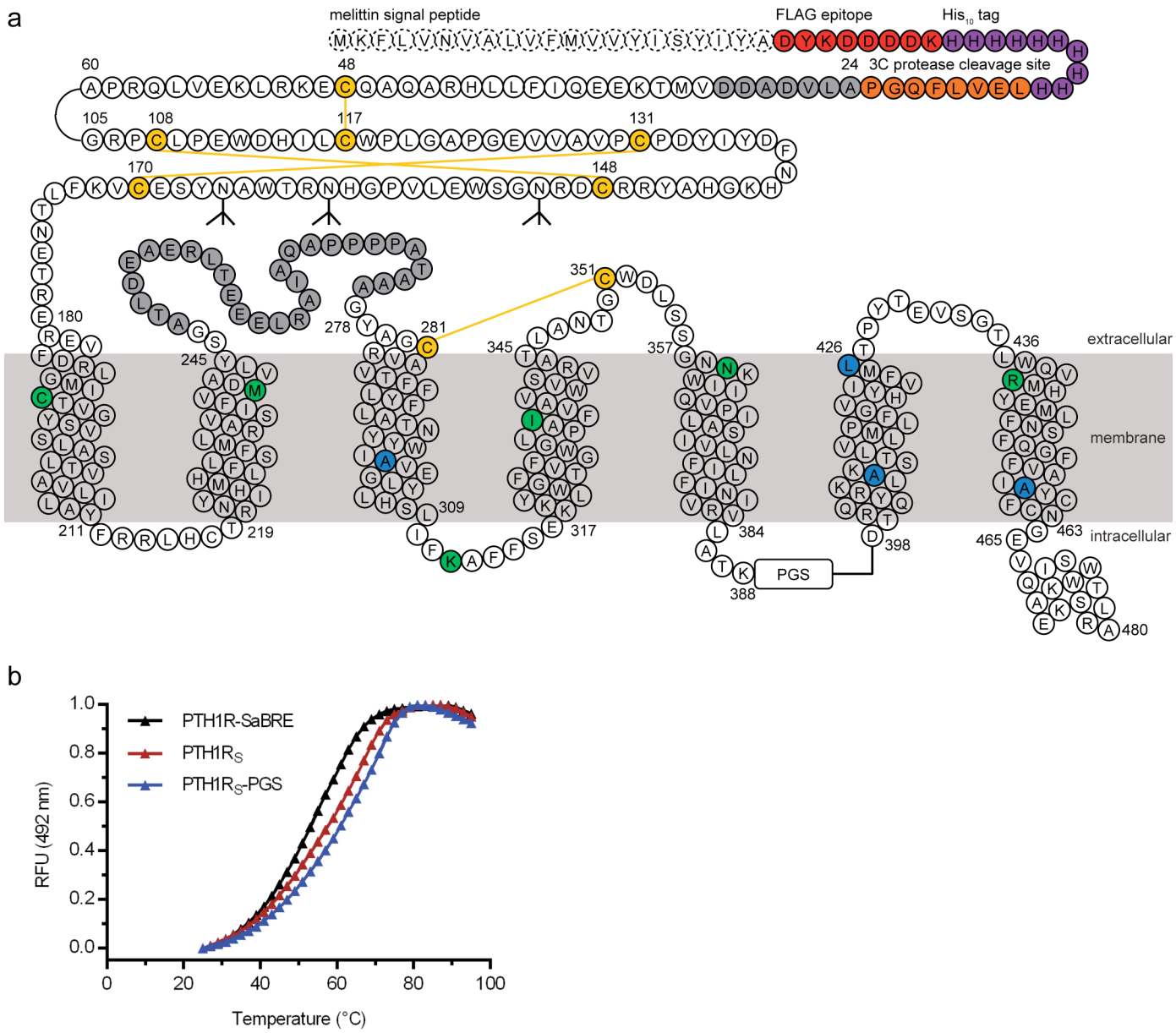

Supplementary Figure 1

Overview of the crystallised PTH1R construct and thermostability of PTH1R mutant TMDs

a, Snake plot of the crystallised ECD-PTH1R$_S$-PGS (PTH1R$_{XTAL}$) construct. The native signal peptide of PTH1R (residues 1-23) was replaced by a melittin signal peptide (dashed circles), followed by a FLAG epitope (red), a His$_{10}$ tag (purple) and a 3C protease cleavage site (orange). Residues 61-104 within the ECD and 481-593 at the receptor C-terminus were deleted. Residues 389-397 of ICL3 were replaced by a PGS fusion. Mutations from directed evolution in *S. cerevisiae* and the additionally introduced stabilising mutations are highlighted in green and blue, respectively. Disulfide bonds are indicated as yellow lines. Glycosylation sites observed in the crystal structure are indicated by a trident. The first and last residues of helices I to VIII are labelled with the residue number. Residues which are not resolved in the crystal structure are shown in grey. **b,** Thermostability assay (CPM) of the TMD of the yeast-evolved PTH1R (PTH1R-SaBRE), the further thermostabilised PTH1R (PTH1R$_S$) and the PTH1R$_S$-PGS fusion (PTH1R$_S$-PGS) bound to [Ac5c$_1$, Aib$_3$, Q$_{10}$, Hrg$_{11}$, A$_{12}$, W$_{14}$]PTH(1-14) (respective melting temperatures are 53.0°C, 57.6°C and 60.9°C).

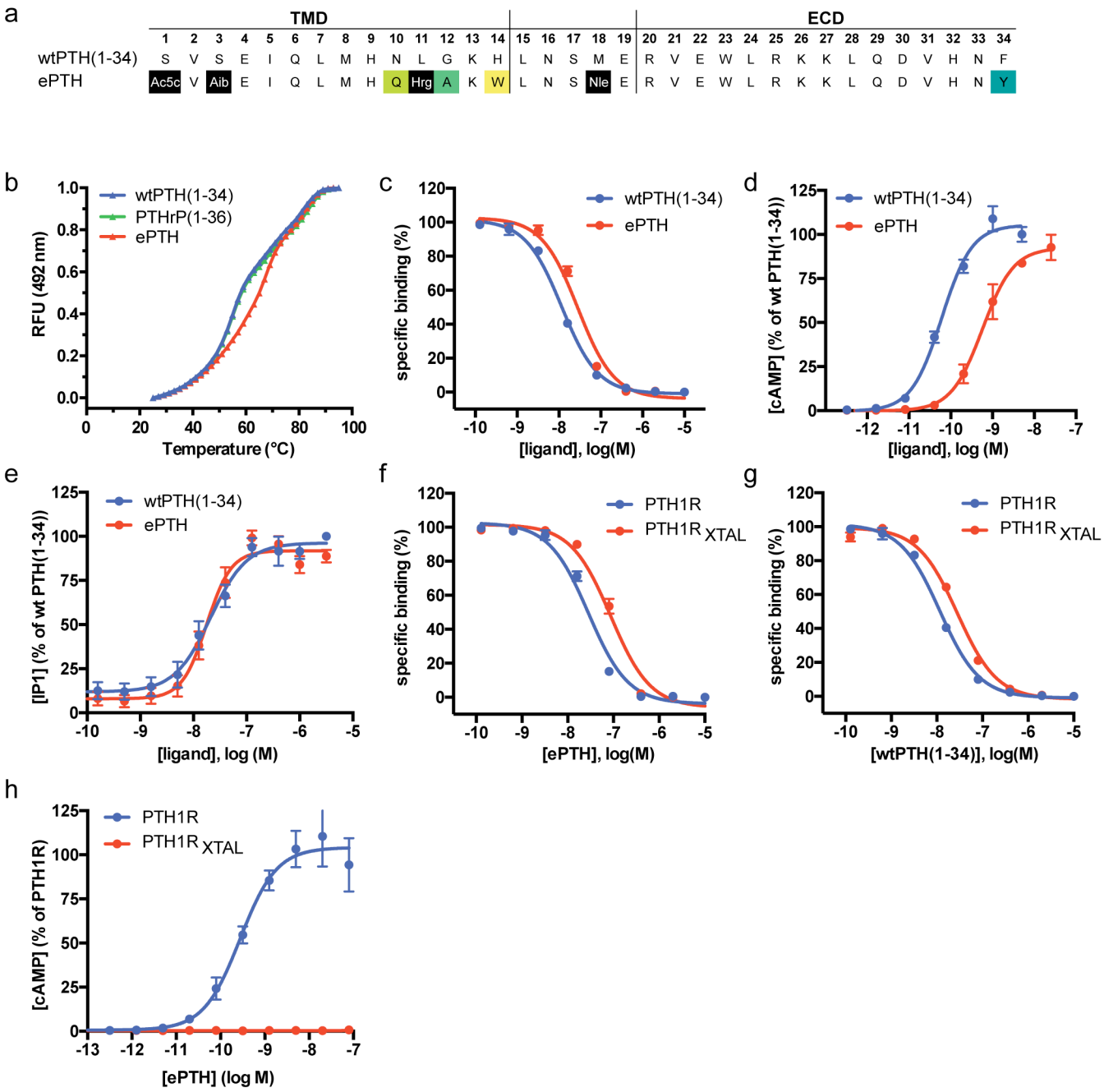

Supplementary Figure 2

Comparison of PTH peptide sequences and in vitro pharmacology of ligands and receptor constructs

a, Sequence alignment of human PTH (wt PTH) and engineered ePTH. Coloured boxes depict sequence changes in comparison to wt PTH, black boxes denote non-natural amino acids. The topology of PTH1R interaction is indicated on top. Ac5c, aminocyclopentane-1-carboxylic acid; Aib, α-aminoisobutyric acid; Hrg, homoarginine; Nle, norleucine. **b,** Thermostability assay (CPM) of the crystallised ECD-PTH1R$_S$-PGS (PTH1R$_{XTAL}$) fusion bound to wt PTH(1-34), wt PTHrP(1-36) and ePTH (respective melting temperatures are 58.0°C, 58.4°C and 65.0°C). Data shown are from a representative experiment. **c,** Binding of PTH-HL$_{647}$ to HEK293T cells expressing wt PTH1R in the presence of different concentrations of unlabelled PTH peptides. **d,** cAMP accumulation measured in HEK293T cells expressing wt PTH1R. **e,** IP1 accumulation measured in HEK293T cells expressing wt PTH1R. **f-g,** Binding of PTH-HL$_{647}$ to HEK293T cells expressing wt PTH1R or the crystallised PTH1R with the PGS fusion (PTH1R$_{XTAL}$) in the presence of different concentrations of unlabelled ePTH (**f**) or wt PTH(1-34) (**g**). **h,** cAMP accumulation measured in HEK293T cells expressing wt PTH1R or the crystallised

PTH1R with the PGS fusion ($PTH1R_{XTAL}$). Data shown in **c-h** are mean values ± SEM from five (**c, f, g**), four (**d-e**) or three (**h**) independent experiments performed in duplicate. The IC_{50} values for **c**, **f**, and **g** are listed in Supplementary Table 2.

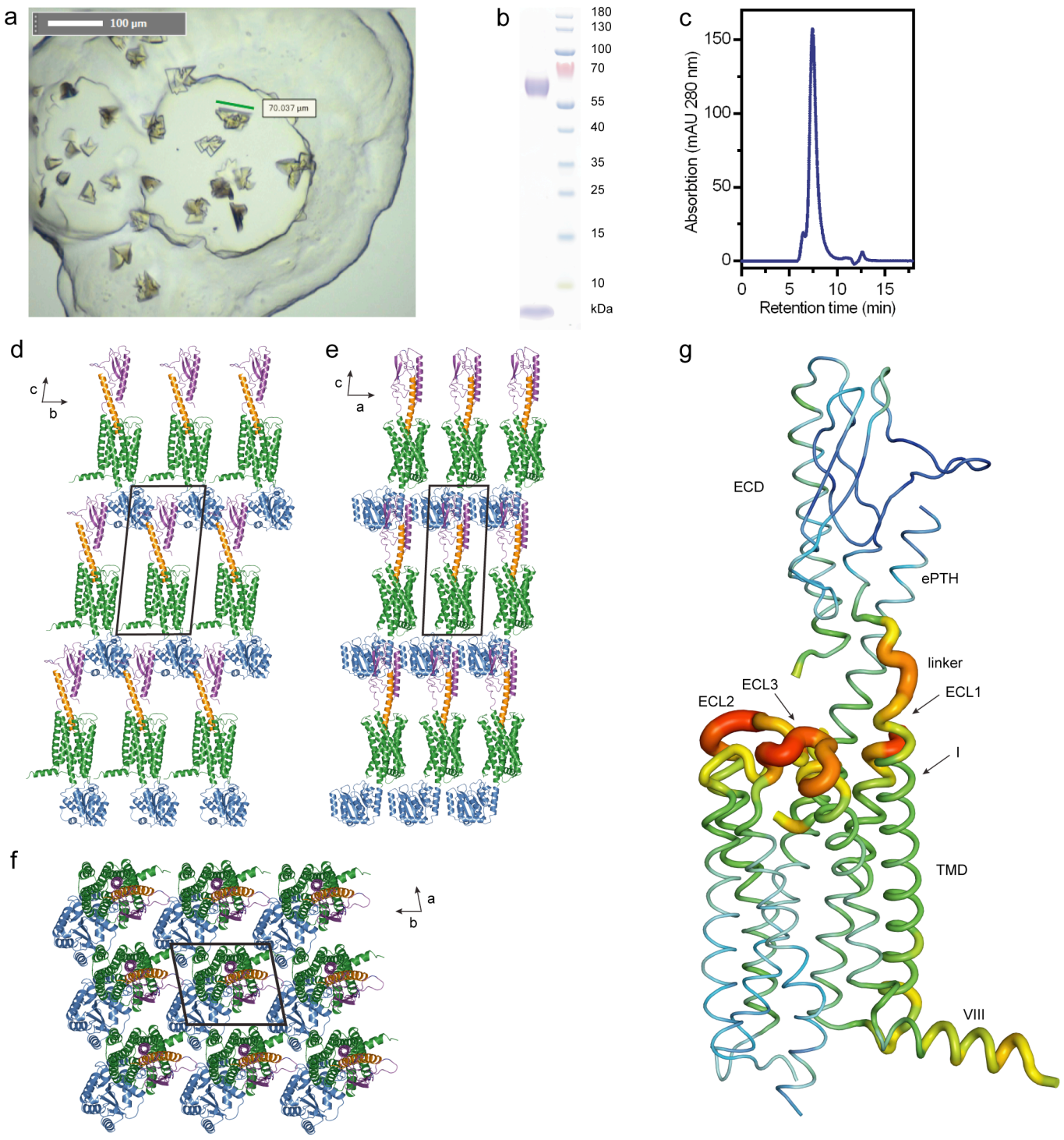

Supplementary Figure 3

PTH1R crystallisation

a, Bright-field image of PTH1R crystals in lipidic cubic phase **b**, SDS-PAGE of purified $PTH1R_{XTAL}$ (upper band with molecular mass 68.3 kDa) bound to ePTH (lower band with molecular mass 4.3 kDa) **c,** Size exclusion profile of $PTH1R_{XTAL}$-ePTH complex on a Nanofilm SEC-250 column (Sepax Technologies) **d-f,** Crystal packing with unit cell indicated in black, axes indicated by arrows (green: TMD, purple: ECD, blue: PGS, orange: ePTH) **d**, view along a axis **e**, view along b axis **f**, view along c axis **g**, B factor putty of PTH1R

(blue: low B factors, red: high B factors). Relatively high B factors are observed within the ECLs and the linker connecting ECD and TMD.

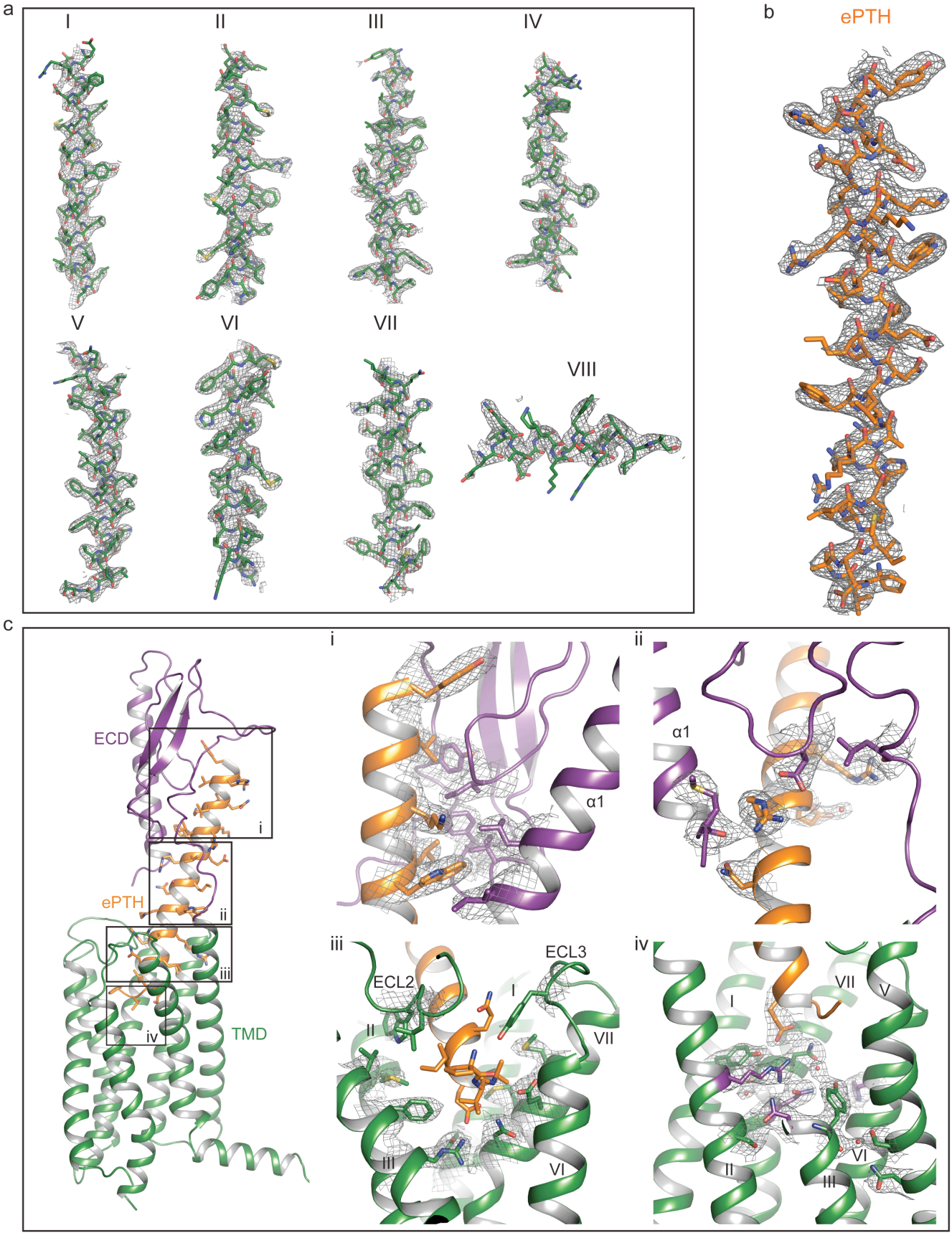
a
I
II
III
IV
V
VI
VII
VIII
b
ePTH
c
ECD
i
ePTH
ii
iii
iv
TMD
i
α1
ii
α1
iii
ECL2
ECL3
I
II
VII
III
VI
iv
I
VII
V
II
VI
III

Supplementary Figure 4

Atomic model of the PTH1R-ePTH complex in the electron density map

a-c, $2F_o$-F_c electron density map contoured at 1.0 σ and model are shown for all seven transmembrane helices, helix VIII and ePTH (**a**,**b**) and the PTH1R-ePTH interacting residues (**c**). Boxes i-iv illustrate the specific regions of ligand interaction with the receptor.

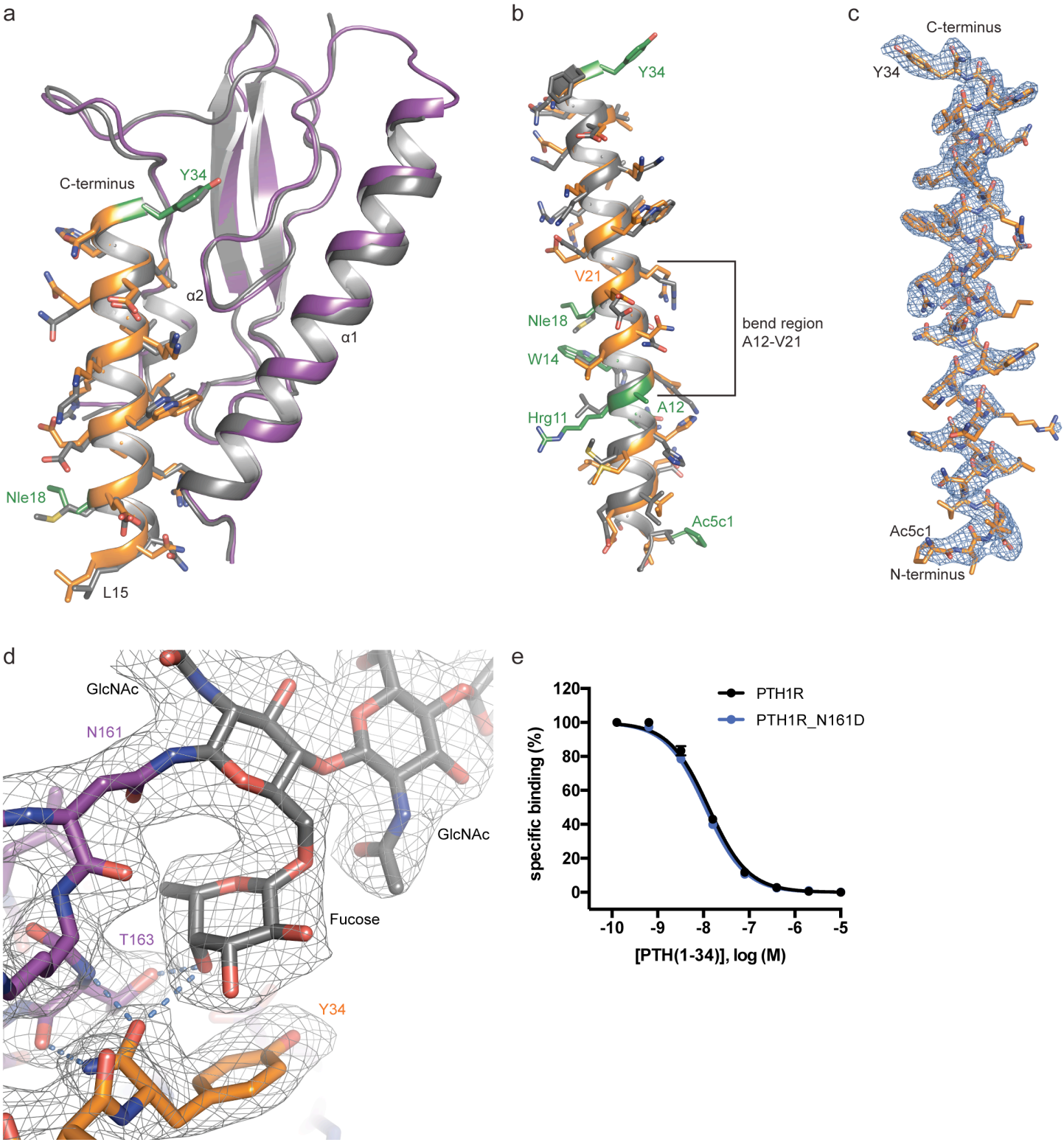

Supplementary Figure 5

Comparison of the structures of wt PTH and ePTH bound to PTH1R and role of glycosylation at N161 on PTH binding

a, Overlay of the crystal structures of ECDs of PTH1R-ePTH (purple and orange) and of the isolated ECD in complex with wt PTH(1-34)

(PDB ID: 3C4M, gray) with ligand residues shown in stick representation. Residues in ePTH differing to wt PTH are highlighted in green. **b**, Superposition of ePTH with the crystal structure of wt PTH(1-34) (PDB ID: 1ET1, gray). **c**, ePTH with Fo-Fc omit density map contoured at 2.5 σ. **d,** ECD of PTH1R with glycosylation (grey) resolved at residue N161 in close proximity to ePTH (orange) shown in sticks. The hydrogen bonds (dashed blue lines) between the amidated peptide C-terminus of Y_{34} and T163 of PTH1R rationalise the reported increase in binding affinity of C-terminal amides over carboxylic acids in PTH(1-34) peptides (Parsons, J. A. et al. *Proc. of the Fifth Parathyroid Conf.*, 33–39 (1975)). $2F_o$-F_c electron density in grey mesh is contoured at 1.0 σ. **e**, Binding of PTH-HL_{647} to HEK293T cells expressing wt PTH1R and the mutant PTH1R_N161D in the presence of different concentrations of unlabelled PTH peptide. Data are shown as mean values ± SEM from n=7 independent experiments performed in duplicate. The IC_{50} values for the wt and PTH1R_N161D are listed in Supplementary Table 2.

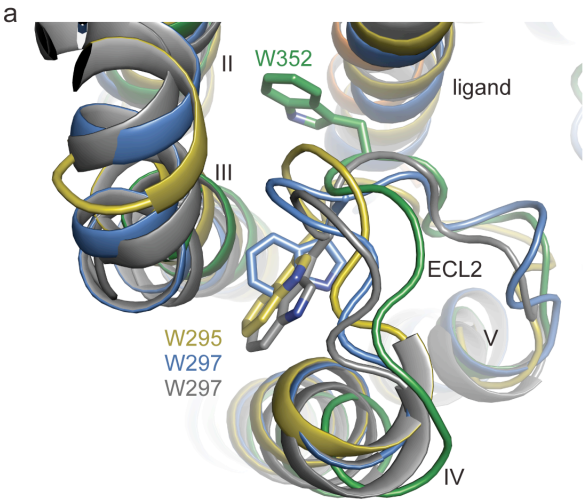

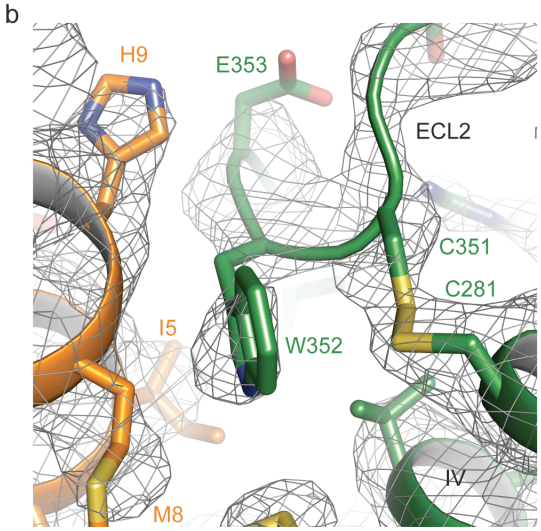

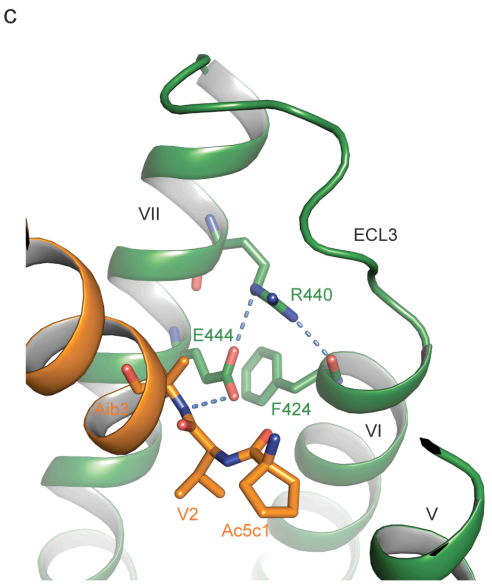

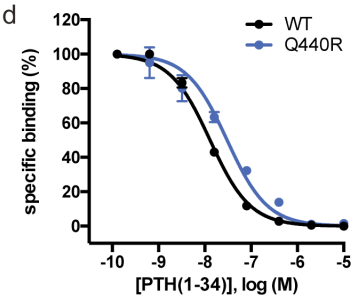

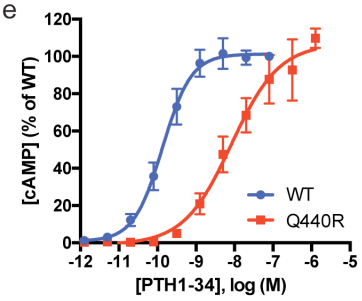

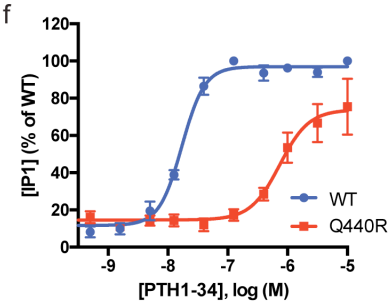

g

	central polar network				receptor activation				P-x-x-G		orthosteric binding pocket					
	2.60	3.43	6.52	7.49	1.47	1.50	3.44	5.50	6.47	6.50	3.29	ECL2	ECL2	7.39	7.42	7.43
PTHR1	R	N	H	Q	Y	S	Y	N	P	G	C	C	W	M	E	M
PTH2R	R	N	H	Q	Y	S	Y	N	L	G	C	C	W	M	E	L
GHRHR	K	N	H	Q	H	S	F	N	P	G	C	C	W	L	E	L
GIPR	R	N	H	Q	Y	S	Y	N	P	G	C	C	W	L	E	I
GLP1R	R	N	H	Q	Y	S	Y	N	P	G	C	C	W	L	E	L
GLP2R	R	N	H	H	Y	S	Y	N	P	G	C	C	W	L	Q	L
GCGR	K	N	H	Q	Y	S	Y	N	P	G	C	C	W	L	D	L
SCTR	R	N	H	Q	Y	S	Y	N	P	G	C	C	W	L	E	L
PAC1R	R	N	H	Q	Y	S	Y	N	P	G	C	C	W	L	E	L
VIPR1	R	N	H	Q	Y	S	F	N	P	G	C	C	W	M	E	L
VIPR2	R	N	H	Q	Y	S	F	N	P	G	C	C	W	I	E	L
CRHR1	R	N	T	Q	H	S	F	N	P	G	C	C	W	I	N	S
CRHR2	R	N	T	Q	H	S	F	N	P	G	C	C	W	I	N	S
CALCR	N	N	Q	Q	H	S	Y	N	P	G	C	C	W	D	M	H
CALCRL	N	N	E	Q	H	S	Y	N	P	G	C	C	W	D	M	H

Supplementary Figure 6

Conserved residues and implication of R440 in ligand binding and receptor activation

a, Extracellular view on the conserved tryptophan in ECL2 of superposed structures of PTH1R-ePTH (green-orange), GCGR-NNC1702 (yellow, PDB ID: 5YQZ), GLP1R-ExP5 (blue, PDB ID: 6B3J) and GLP1R-GLP1 (grey, PDB ID: 5VAI) complexes. While this tryptophan is positioned between transmembrane helices III and IV in the structures of the other peptide-bound class B GPCRs, it is found in a different orientation packed against the ligand in the PTH1R-ePTH complex. **b,** The distinct orientation of W352 in PTH1R is defined by the clear side chain electron density in the $2F_o$-F_c map contoured at 1.0 σ. **c,** The stabilising mutation $R440^{7.38}$ ($Q440^{7.38}$ in wt PTH1R) forms a hydrogen bonding network to ePTH via $E444^{7.42}$ and to the backbone oxygen of $F424^{6.56}$ at the extracellular end of helix VI. **d,** Binding of PTH-HL_{647} to HEK293T cells expressing wt or mutated PTH1R in the presence of different concentrations of unlabelled PTH peptides. Mutation of $Q440^{7.38}$ to R largely retains ligand binding, whereas disruption of the hydrogen bond to $E444^{7.42}$ by introduction of small, apolar side chain residues severely reduces ligand binding (Lee, C. et al. *Mol. Endocrinol.* **9,** 1269–1278 (1995)). **e-f,** Normalised concentration-response curves for cAMP (**e**) or IP1 (**f**) accumulation, measured in HEK293T cells expressing wt or mutant PTH1R. In contrast to $Q440^{7.38}$ of wt PTH1R, the extended sidechain of $R440^{7.38}$ stabilises the top of helix VI by an additional hydrogen bond to $F424^{6.56}$, and thus strongly reduces receptor activation, which requires conformational rearrangements at the extracellular end of helix VI. **g,** amino acid alignment of specific conserved residues of 15 human class B GCPRs grouped into those of the central polar network, those involved in receptor activation, the P-x-x-G motif and in the orthosteric binding pocket (Wootten numbering is given as a superscript). Data in **d-e** are shown as mean values ± SEM from seven (**d**), five (**e**) or three (**f**) independent experiments performed in duplicate. The IC_{50} values of **d** are listed in Supplementary Table 2.

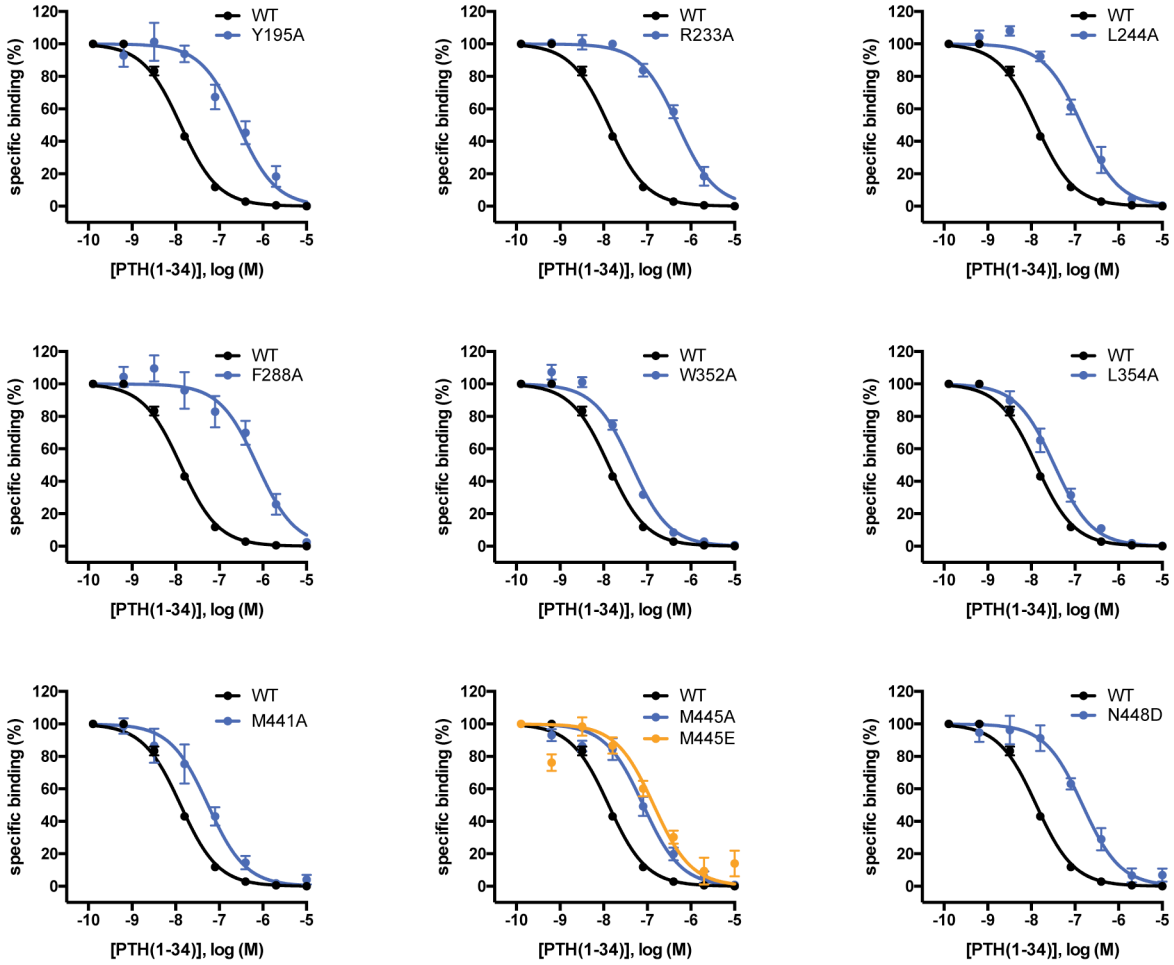

Supplementary Figure 7

Binding of PTH(1-34) to wild-type and mutant variants of PTH1R

Binding of PTH-HL_{647} to HEK293T cells expressing wild-type and mutated PTH1R variants in the presence of different concentrations of unlabelled wt PTH(1-34) as a competitor. Data are shown as mean values ± SEM from 4-12 independent experiments performed in duplicate. The corresponding IC_{50} values and numbers of independent experiments for wt and mutant PTH1Rs are listed in Supplementary Table 2.

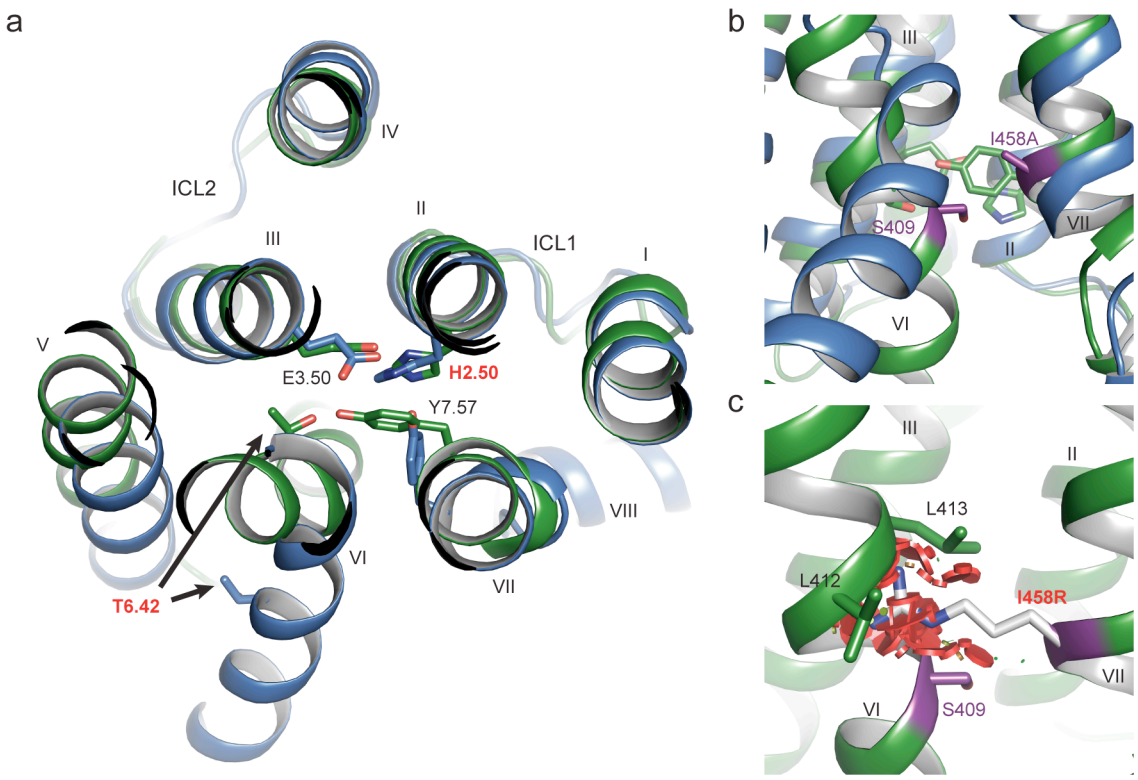

Supplementary Figure 8

Jansen's Metaphyseal Chondrodysplasia-related mutations at the conserved HETX motive result in constitutive PTH1R activation.

a, Extracellular view on the class B conserved HETX motive of superposed PTH1R (green) and activated GLP1R (blue, PDB ID: 5VAI). In the active state receptor, $T^{6.42}$ is removed from the network due to rearrangements in transmembrane helix VI. Residues associated with Jansen's Metaphyseal Chondrodysplasia are highlighted in red. **b-c,** The thermostabilising mutation $I458^{7.56}A$ in the crystallised PTH1R and the Jansen's Metaphyseal Chondrodysplasia-related mutation $I458^{7.56}R$ facing towards $S409^{6.41}$ are located close to the HETX motive (view from the membrane). The bulky sidechain of $I458^{7.56}R$ clashes (indicated by red disks) with helix VI in the inactive receptor state (representative rotamer from PyMOL Mutagenesis Wizard shown).

Supplementary Table 1 | Interactions between ePTH and PTH1R

Residue in ePTH	Residue in PTH1R	Interaction*
$Ac5c_1$	$Q364^{5.40}$	
	$Y429^{ECL3}$	Hydrogen bond
V_2	$F288^{3.36}$	
	$L292^{3.40}$	
Aib_3	$M441^{7.39}$	
	$E444^{7.42}$	Hydrogen bond to peptide backbone
	$M445^{7.43}$	
E_4	$Y195^{1.47}$	Hydrogen bond
	$R233^{2.60}$	Hydrogen bond
	$F288^{3.36}$	
	$N448^{7.46}$	Hydrogen bond
I_5	$M240^{2.67}$	
	$V285^{3.33}$	
	$F288^{3.36}$	
	$W352^{ECL2}$	
	$L354^{ECL2}$	
Q_6	$Y429^{ECL3}$	
L_7	$L187^{1.39}$	
	$G188^{1.40}$	
M_8	$M240^{2.67}$	
	$D241^{2.68}$	
	$W352^{ECL2}$	
H_9	$D353^{ECL2}$	
Q_{10}	$F184^{1.36}$	
Hrg_{11}	$F184^{1.36}$	
	$L244^{2.71}$	
	$Y245^{2.72}$	Hydrogen bond
A_{12}	$W352^{ECL2}$	
W_{14}	$E180^{1.32}$	
	$R181^{1.33}$	
	$F184^{1.36}$	
N_{16}	$M32^{ECD}$	Hydrogen bond to peptide backbone
	$N33^{ECD}$	

E_{19}	$K34^{ECD}$	
R_{20}	$M32^{ECD}$	Hydrogen bond to peptide backbone
	$Q37^{ECD}$	
	$Y136^{ECD}$	
	$D137^{ECD}$	Salt bridge
V_{21}	$D137^{ECD}$	
W_{23}	$K34^{ECD}$	
	$I35^{ECD}$	
	$N37^{ECD}$	
	$I38^{ECD}$	
L_{24}	$I135^{ECD}$	
	$F138^{ECD}$	
	$L174^{ECD}$	
R_{25}	$L174^{ECD}$	Hydrogen bond to peptide backbone
K_{27}	$L41^{ECD}$	
	$I115^{ECD}$	
L_{28}	$I115^{ECD}$	
	$F138^{ECD}$	
D_{30}	$H114^{ECD}$	
V_{31}	$I115^{ECD}$	
	$Y167^{ECD}$	
Y_{34}	$D113^{ECD}$	
	$H114^{ECD}$	
	$R162^{ECD}$	
	$T163^{ECD}$	Hydrogen bond
C-terminal amide	$T163^{ECD}$	Hydrogen bond to peptide backbone

* Polar interactions are listed

Supplementary Table 2 | Binding of PTH(1-34) to wild-type and mutated PTH1R variants.

construct	IC_{50} (nM)	B_{30nM} (% of WT)	surface expression (% of WT)	*n*
wt	13.0±0.9	100	100	12
N161D	11.0±0.5	76.9±9.4	97±5	7
F184A	*n.b.*	25.5±5.7	142±3	4
Y195A	271±43.7	14.3±2.0	89±9	4
R233A	501±40	15.1±1.9	167±20	4
L244A	143±19	29.7±2.0	117±6	9
F288A	740±119	16.7±2.0	132±8	9
W352A	36.9±4.7	33.2±1.5	91±5	9
L354A	43.7±6.0	29.1±4.7	99±7	4
Q440R	30.3±4.5	29.3±2.8	117±4	6
M441E	*n.b.*	11.6±2.3	106±5	4
M441A	55.1±5.8	25.9±2.4	90±12	4
M445A	80.5±10.8	22.9±2.7	113±5	4
M445E	140.0±38.6	12.7±1.4	126±8	4
N448D	149±13	17.6±1.5	105±5	4
$PTH1R_{XTAL}$	28.2±3.8	399±5	433±52	5

Competition binding data of PTH(1-34) to PTH1R constructs as described in Supplementary Fig. 7. Cell surface expression was obtained by measuring fluorescence emission of SNAP-Lumi4-Tb-labeled receptors in the absence of ligand. B_{30nM} is the observed binding (with unspecific binding subtracted) of 30 nM labelled ligand. All values are expressed as mean ± SEM of the indicated number of independent experiments performed in duplicate. *n.b.,* no binding.